HOKKAIDO UNIVERSITY

Title	Catalytic Decomposition of Pyridine with Goethite-Rich Limonite in the Coexistence of Fuel Gas or Coke Oven Gas Components
Author(s)	Ogawa, Ayumu; Mochizuki, Yuuki; Tsubouchi, Naoto
Citation	ISIJ International, 56(7), 1132-1137 https://doi.org/10.2355/isijinternational.ISIJINT-2016-052
Issue Date	2016-07-15
Doc URL	https://hdl.handle.net/2115/79333
Rights	著作権は日本鉄鋼協会にある
Type	journal article
File Information	ISIJ Int. 56(7)_ 1132-1137 (2016).pdf

Hokkaido University Collection of Scholarly and Academic Papers : HUSCAP

ISIJ International, Vol. 56 (2016), No. 7, pp. 1132–1137

Catalytic Decomposition of Pyridine with Goethite-Rich Limonite in the Coexistence of Fuel Gas or Coke Oven Gas Components

Ayumu OGAWA, Yuuki MOCHIZUKI and Naoto TSUBOUCHI*

Center for Advanced Research of Energy and Materials, Faculty of Engineering, Hokkaido University, Kita 13 Nishi 5, Kita-ku, Sapporo, 060-8628 Japan.

(*Received on January 29, 2016; accepted on March 28, 2016*)

Catalytic performance of limonite in the decomposition of 100 ppmv pyridine (C_5H_5N) in the coexistence of fuel gas or coke oven gas (COG) components has been studied mainly with a cylindrical quartz reactor at 750–850°C under a high space velocity of 51 000 h^{-1} to develop a novel hot gas cleanup method of removing the nitrogen in tar as N_2. The limonite catalyst achieves the almost complete decomposition of C_5H_5N in He at 500–850°C and gives a high N_2 yield of more than 85 N% at 500°C. When the decomposition run is performed in the presence of fuel gas or COG components, the coexistence of 20% CO/10% H_2 at 750°C or 50% H_2/30% CH_4/5% CO at 850°C deactivates the limonite with remarkable formation of deposited carbon. On the other hand, the addition of a small amount of H_2O or CO_2 to these atmospheres can improve the catalytic activity without carbon deposition. When 3% H_2O or 10% CO_2 is added to 20% CO/10% H_2, C_5H_5N conversion and N_2 yield at 750°C become 80–95% and 65–80 N%, respectively, and the extent of the improvement is larger with the CO_2 than with the H_2O. The addition of 5% CO_2 to 50% H_2/30% CH_4/5% CO also restores the conversion or the yield at 850°C to the high level of about 90% or 60–70 N%, respectively, and both values at 950°C are comparable to those at 500°C in inert gas.

KEY WORDS: hot gas cleanup; pyridine decomposition; N_2 formation; limonite; fuel gas; coke oven gas.

1. Introduction

Advanced integrated gasification combined cycle (A-IGCC) and fuel cell (A-IGFC) systems are expected to be among the most environmentally acceptable power-generating technologies from coal. A-IGCC and A-IGFC are estimated to achieve high generation efficiencies of more than 57 and 65%, respectively, which corresponds to a reduction of greater than 30% of CO_2 emissions compared to current pulverized coal-fired plants.[1)] Coal-derived fuel gas is composed mainly of syngas ($CO/H_2 = 2$), with low concentrations of CO_2, CH_4 and H_2O.[2–5)] Undesirable impurities, such as hydrogen halide, H_2S, COS, NH_3, HCN, alkali metals and trace elements, are also included in raw fuel gas.[2–5)] Cold gas cleaning methods using Venturi water scrubbers and selective amine-based absorbents are conventional technologies to efficiently remove these solid and gaseous impurities from fuel gas before a gas combustion process with gas turbine or fuel cell.[6–8)] However, a hot gas cleanup method that purifies fuel gas at temperatures of $\geq$ 300°C can reduce the loss of heat energy of the hot raw gas (>700°C) and high capital cost for large waste water treatment facilities used in wet processes.[1,3,4,9,10)]

Coke oven gas (COG) produced during coal carbonization is generally used as a fuel source for coke ovens and other combustion units in ironworks, and it has recently attracted much attention as a low cost source of hydrogen.[11)] In conventional processes, the hot raw COG (>800°C) must be quenched to near room temperature using aqueous ammonia solution to remove tarry materials contained in COG.[11)] On the other hand, the catalytic or noncatalytic reforming of COG is a promising technology effectively utilizing heat energy of the hot COG.[12–15)] Upon coal carbonization, part of the nitrogen present in coal is retained in the solid phase, and the rest is released as volatile-N (N_2, NH_3, HCN and tar-N).[16)] It is well-known that NH_3, HCN and tar-N not only serve as a source of NO_x but also poison catalyst materials used for COG reforming.

Our research group has been working on the decomposition of NH_3 or model tar-N compounds (pyridine or pyrrole) using inexpensive iron catalysts.[17–26)] We have found that fine particles of metallic iron (α-Fe) formed from low-valued iron ore (limonite) show higher activity in the decomposition of NH_3 compared to Ni-, Cu-, Mo- and Ru-based catalysts reported previously.[2,19–23,26)] The limonite can achieve almost complete decomposition of 2 000 ppmv NH_3 diluted with inert gas at 500°C[19)] and exhibit stable activity in the presence of fuel gas components at 850°C.[20–23,26)] We have recently shown that limonite-derived α-Fe can give a N_2 yield of more than 80% in the decomposition of 100 ppmv pyridine (C_5H_5N) in inert He at 500°C under a high space velocity of 51 000 h^{-1}.[25)] In this paper, therefore, we focus on investigating the catalytic performance of an Australian limonite in the decomposition of C_5H_5N in the coexistence of fuel gas or COG components to develop a novel gas

* Corresponding author: E-mail: tsubon@eng.hokudai.ac.jp
DOI: http://dx.doi.org/10.2355/isijinternational.ISIJINT-2016-052

© 2016 ISIJ

cleaning method for removing tar-N as N_2.

2. Experimental

2.1. Catalyst Material and Preparation

An Australian natural limonite ore comprising about 70% of goethite (α-FeOOH) was employed as a catalyst precursor in the present study. The metal composition of the limonite was: Fe, 44; Si, 9.4; Al, 7.2; Mg, 0.15; Ca, 0.07 mass%-dry.[25] The as-received limonite was sieved to select the 250–500 μm size fraction, and the Brunauer-Emmett-Teller (BET) specific surface area was measured at 40 m^2/g.[25]

2.2. Pyridine Decomposition

Catalytic decomposition of C_5H_5N was carried out with a cylindrical fixed-bed quartz reactor (8 mm i.d.) under ambient pressure. The details of the experimental apparatus have been described elsewhere.[17] The temperature was controlled by a K-type thermocouple attached to the exterior surface of the reactor. Approximately 0.25 g of the limonite was first charged into the reactor with quartz wool, and a flow of high-purity He (>99.99995%) was then passed through the reactor until the concentration of N_2 in the experimental system was decreased to less than 20 ppmv. The height of catalyst bed in the reactor was about 7.0 mm. After taking precautions against leakage, the reactor was heated electrically up to 500°C. At this temperature, the He was replaced with high-purity H_2 (>99.9999%), and the catalyst material was reduced with the H_2 for 2 h. The reduced limonite catalyst is present as α-Fe with the average crystalline size of 25 nm as mentioned later (Section 3.4). After the reduction pretreatment, the atmosphere was restored to the He, and the reactor was held at a temperature between 300–950°C. The C_5H_5N decomposition experiment began by passing 100 ppmv C_5H_5N diluted with the He, simulated fuel gas (20% CO/10% H_2, 20% CO/10% H_2/3% H_2O and 20% CO/10% H_2/10% CO_2) or simulated COG (50% H_2/30% CH_4/5% CO and 50% H_2/30% CH_4/5% CO/5% CO_2) over the catalyst bed. The space velocity was maintained at 51 000 h^{-1} throughout the run.

2.3. Gas Analysis

The amount of N_2 produced in the decomposition of C_5H_5N was measured at 3 min intervals with a high-speed micro gas chromatograph (Agilent) equipped with a thermal conductivity detector. Concentrations of C_5H_5N, NH_3 and HCN were determined at 2 min intervals with a photoacoustic multigas monitor (Innova). In the C_5H_5N decomposition runs in the coexistence of CO, CO_2, CH_4 and/or H_2O, the C_5H_5N, NH_3 and HCN were analyzed independently by the Gastec standard detector tube (Gastec) because the analytical accuracy of the multigas monitor may be deteriorated by CO, CO_2, CH_4 and/or H_2O. The amount of C_5H_5N fed was calculated using the concentrations of C_5H_5N before and after reaction. The yield of N_2, HCN or NH_3 was estimated using the amounts of both C_5H_5N fed and N_2, HCN or NH_3 formed, respectively, and it was expressed in percent on a nitrogen basis.

2.4. Catalyst Characterization

The powder X-ray diffraction (XRD) (Shimadzu) measurements of catalyst samples as received, after H_2 reduction and after C_5H_5N decomposition were performed with Mn-filtered Fe-Kα radiation. The average crystallite size of α-Fe was determined by the Debye-Scherrer method. To avoid rapid oxidation of α-Fe particles upon exposure to laboratory air, the limonite after H_2 reduction or C_5H_5N decomposition was passivated using 2% O_2/He at room temperature and then recovered from the reactor.[19]

3. Results and Discussion

3.1. Decomposition of Pyridine in Inert Gas

The results for the decomposition of 100 ppmv C_5H_5N in inert He with the limonite catalyst have mostly been shown elsewhere[25] and are thus summarized simply in **Table 1**. In a blank experiment with quartz wool alone at 850°C, C_5H_5N conversion was less than 1%. At 300–500°C, the conversion and N_2 yield after 4 h increased with increasing temperature in many cases (Table 1). The reason for it may be that the extent of the transformation of C_5H_5N into N_2 is larger at a higher temperature. The limonite also provided a high N_2 yield of more than 80 N% for at least 10 h at 500°C.[25] At a temperature of more than 600°C, although the conversion was greater than 99% during 4 h reaction, the yield decreased gradually after 3 h (Table 1). The catalysts after reaction at 300–500°C were apparently homogeneous, however, the samples after the reaction at ≥ 600°C were divided into two layers. According to XRD analyses, the upper layer was rich in crystallized carbon and cementite (Fe_3C) derived from C_5H_5N decomposition, whereas the lower layer was rich in α-Fe formed upon the H_2 reduction. Thus, the decrease in N_2 yield observed at ≥ 600°C may be ascribed to the adsorption of C_5H_5N onto the carbon deposited at the upper layer and/or the transformation of catalytically active α-Fe into the carbide species. We have recently shown that the limonite-catalyzed N_2 formation from C_5H_5N in inert gas takes place via a cycle mechanism involving α-Fe and the nitride species (for example, Fe_2N, Fe_3N and Fe_4N).[25] When N_2 yields at 600–850°C were compared, as provided in Table 1, the yield was larger at a higher temperature. The reason may be that the extent of the transformation of nitrogen element incorporated in C_5H_5N-drived carbona-

Table 1. C_5H_5N conversion and yield of N_2, HCN or NH_3 in the limonite-catalyzed decomposition of C_5H_5N in inert He at different temperatures.

Temperature (°C)	C_5H_5N conversion (%)[a]	N_2 yield (N%)[a]	HCN yield (N%)[a]	NH_3 (N%)[a]	Ref. no
300	5	<1	5	<1	25)
350	7	1	3	<1	25)
400	7	7	3	<1	25)
450	88	76	2	<1	25)
500	>99	85	2	<1	25)
600	>99	72	2	<1	This work
750	>99	74	3	<1	This work
850	>99	78	2	<1	This work

[a]After 4 h reaction.

© 2016 ISIJ

ceous materials into N_2 is larger at a higher temperature.[25] The yield of HCN or NH_3 was less than 5 N% and 1 N%, respectively, under all conditions. It has been reported that most of the nitrogen in pyridine is decomposed into cyanide species at above 800°C.[27] It might thus be possible that the limonite catalyzed the decomposition of C_5H_5N into HCN, which might subsequently be transformed into N_2.[24]

3.2. Decomposition of Pyridine in the Coexistence of Fuel Gas Components

Figure 1 presents the effect of the limonite catalyst on C_5H_5N decomposition in the presence of syngas (20% CO/10% H_2) at 750°C. C_5H_5N conversion after 2 h reaction was as high as >95%, which was comparable to the value in inert He (Table 1). On the other hand, N_2 yield decreased to less than 30 N% after 2 h. The yields of NH_3 and HCN were always less than 10 N%. Since the formation of CO_2 and carbonaceous materials occurred under the present conditions, the catalyst deactivation observed in Fig. 1 may be ascribed to the carbon deposition by the disproportionation of CO in the syngas (Eq. (1)).

$$2CO \rightarrow C + CO_2 \quad \text{..... (1)}$$

On the other hand, the high C_5H_5N conversion in Fig. 1 may originate from the adsorption of C_5H_5N onto the deposited carbon formed during the reaction.

As well-known, fuel gas from air-blown coal gasifiers contains small amounts of H_2O and CO_2.[2,3,23] Thus, the effect of H_2O or CO_2 addition to syngas on C_5H_5N decomposition was investigated.

Figure 2 shows the influence of 3% H_2O addition on C_5H_5N decomposition under flowing 20% CO/10% H_2 at 750°C. The comparison with Fig. 1 revealed that the co-feeding of the H_2O could maintain the C_5H_5N conversion or N_2 yield at the level of more than 80% or about 65 N%, respectively. NH_3 yield was approximately 20 N% during 4 h reaction, and HCN was always negligibly small. Although the C_5H_5N conversion was about 95% in He, the value lowered to 80–90% with the co-feeding of the H_2O. In addition, N_2 yield after 1 h reaction also decreased from 75% in He (Fig. 1) to 65% in the case of H_2O co-feeding (Fig. 2). The reason for it may be that part of nitrogen in C_5H_5N is transformed into unmeasured N-species other than the N-forms mentioned above. **Figure 3** presents the concentration of CO_2 evolved in the runs shown in Figs. 1 and 2. Approximately 1 000–2 000 ppmv of CO_2 was produced during C_5H_5N decomposition under flowing syngas alone. This result points out that Eq. (1) occurs significantly. In the coexistence of the H_2O, as seen in Fig. 3, the concentration at a steady state was about 7 000 ppmv, which was much higher than that without the H_2O added. It is thus likely that the following CO-H_2O reaction (Eq. (2)), that is, the water gas shift reaction, takes place in the process of C_5H_5N decomposition.

$$CO + H_2O \rightarrow CO_2 + H_2 \quad \text{..... (2)}$$

No significant carbon formation was also observed after the decomposition reaction in the H_2O-containing syngas. This may be ascribed to the suppression of carbon deposition (Eq. (1)) by the CO_2 produced through Eq. (2) and/or the occurrence of the reaction (Eq. (3)) of deposited carbon with the H_2O added.

$$C + H_2O \rightarrow CO + H_2 \quad \text{..... (3)}$$

It has recently been shown that limonite-catalyzed steam gasification of coal chars can proceed remarkably around 800°C.[28]

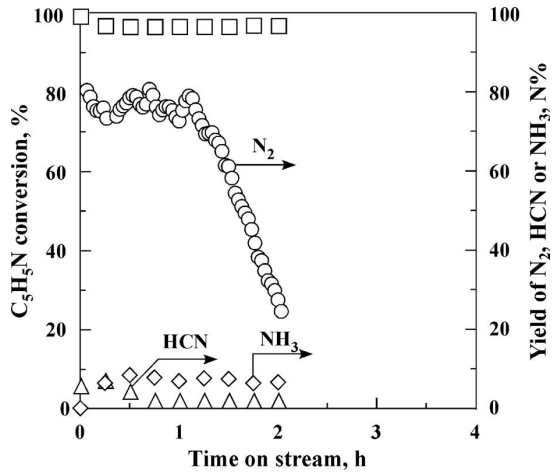


Fig. 1. Influence of the coexistence of syngas (20% CO/10% H_2) on C_5H_5N decomposition with limonite at 750°C.

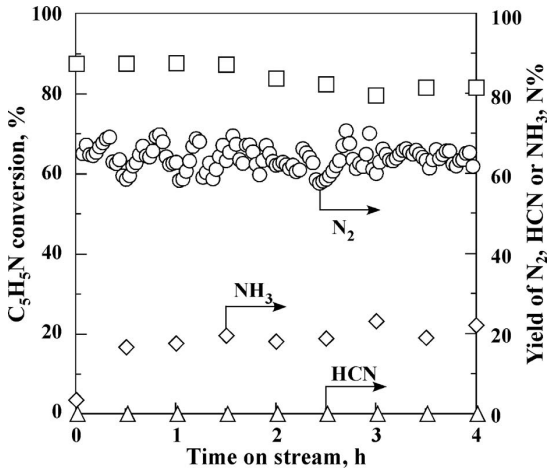


Fig. 2. Effect of 3% H_2O addition on C_5H_5N decomposition under flowing 20% CO/10% H_2 at 750°C.

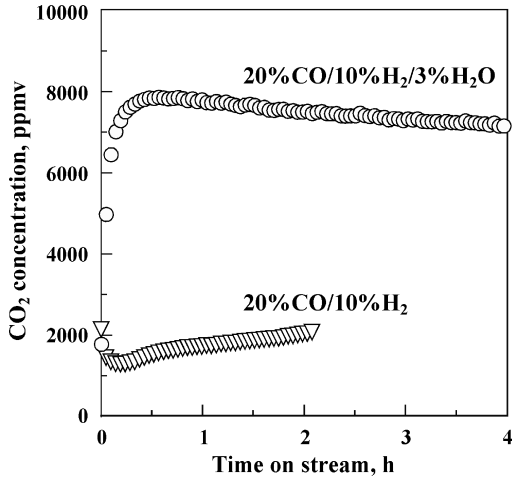


Fig. 3. Concentration of CO_2 evolved during C_5H_5N decomposition at 750°C in the coexistence of syngas alone or 3% H_2O-containing syngas.

© 2016 ISIJ

Figure 4 shows the results under flowing 10% CO_2-containing syngas. When the CO_2 was added to 20% CO/10% H_2, C_5H_5N conversion or N_2 yield after 4 h was almost the same level as the corresponding value (Table 1) observed at 500°C in inert He. NH_3 and HCN were ≤ 5 N% and almost zero, respectively. The co-feeding of a higher concentration of CO_2 may lower the driving force for Eq. (1) to a larger extent so that the CO_2 added may improve the activity of the limonite catalyst more effectively compared with 3% H_2O addition (Fig. 2). When the decomposition run given in Fig. 4 was carried out at 650°C, the catalytic performance of the limonite was decreased by carbon deposition, which may come from a higher driving force ($\Delta G = -2.1$ kcal/mol) for Eq. (1) at 650°C compared with that ($\Delta G = 2.1$ kcal/mol) at 750°C. The catalytic activity in the CO_2-containing syngas at 850°C was almost the same level as that (Fig. 4) at 750°C. It is thus probable that the addition of 10% CO_2 to syngas can restore the catalytic performance of the limonite to the high level at ≥ 750°C.

3.3. Decomposition of Pyridine in the Coexistence of Coke Oven Gas Components

It is well-known that a typical COG is composed of 54–59% H_2, 24–28% CH_4, 4–7% CO, 3–5% N_2 and 1–3% CO_2 with impurities.[15] The present section therefore focuses on investigating the effect of the coexistence of H_2, CH_4, CO and/or CO_2 on the limonite-catalyzed C_5H_5N decomposition.

Figure 5 presents the effect of the limonite catalyst on C_5H_5N decomposition in the presence of 50% H_2/30% CH_4/5% CO at 850°C. C_5H_5N conversion was about 90% during 1 h reaction, whereas N_2 yield decreased with increasing time on stream beyond 30 min to be less than 30 N% after 1 h. On the other hand, HCN and NH_3 yields were almost constant for 1 h. The difference in the behavior of N_2, HCN and NH_3 formation may occur due to the transformation of C_5H_5N into unmeasured N-species, because the catalyst used in this atmosphere was covered with a large amount of deposited carbon, which is likely to be derived from CH_4 (Eq. (4)) and/or CO (Eq. (1)) in the atmosphere. It is probable that the remarkable occurrence of carbon formation is the main reason for the catalyst deactivation observed in Fig. 5.

$$CH_4 \rightarrow C + 2H_2 \quad \text{..... (4)}$$

Figure 6 shows the influence of 5% CO_2 addition on C_5H_5N decomposition under flowing 50% H_2/30% CH_4/5% CO at 850°C. The added CO_2 could improve the catalytic activity of the limonite remarkably compared with the observation (Fig. 5) without CO_2 added. The conversion was stable at about 90%, and N_2 yield was 60–70 N% during 4 h reaction. NH_3 and HCN were also about 20 N% and almost zero, respectively. No significant carbon deposition was observed under the conditions applied. It is probable that the decrease in carbonaceous materials by CO_2 addition is responsible for the activity improvement observed in Fig. 6. When the temperature was decreased to 750°C, the conversion decreased steeply at the initial step of the reaction to be about 60% after 1 h. At 950°C, on the other hand, the conversion was as high as >95% for 4 h, and N_2 was stable at about 80 N%. Thermodynamic calculations indicate that the driving force for the methane decomposition reaction (Eq. (4)) described above is greater at a higher temperature ($\Delta G = -5.2$ kcal/mol at 750°C, −7.8 kcal/mol at 850°C and −10 kcal/mol at 950°C). However, the catalytic activity of the limonite was higher at ≥ 850°C than at 750°C. The reason for this difference is not clear at present, but the occurrence of the Boudouard reaction (the reverse reaction

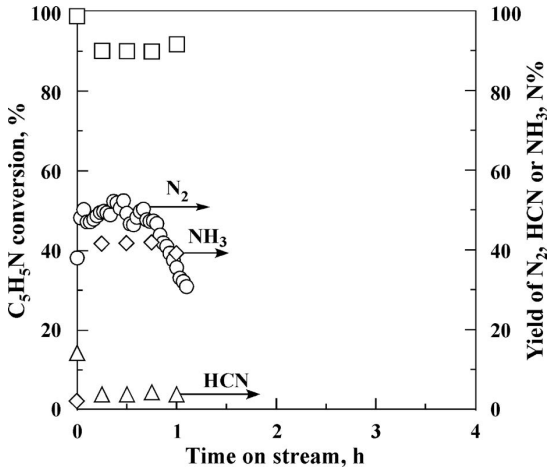


Fig. 5. Influence of the coexistence of 50% H_2/30% CH_4/5% CO on C_5H_5N decomposition with limonite at 850°C.

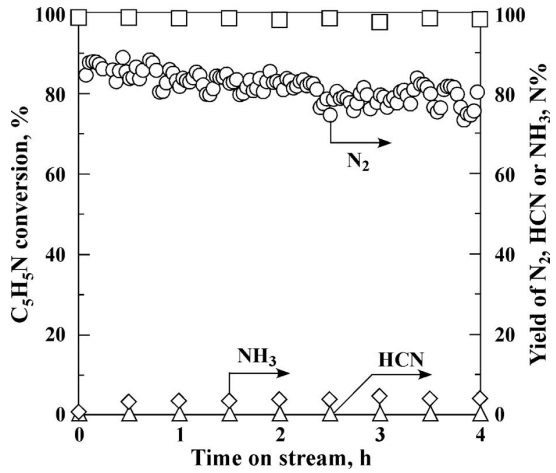


Fig. 4. Effect of 10% CO_2 addition on C_5H_5N decomposition under flowing 20% CO/10% H_2 at 750°C.

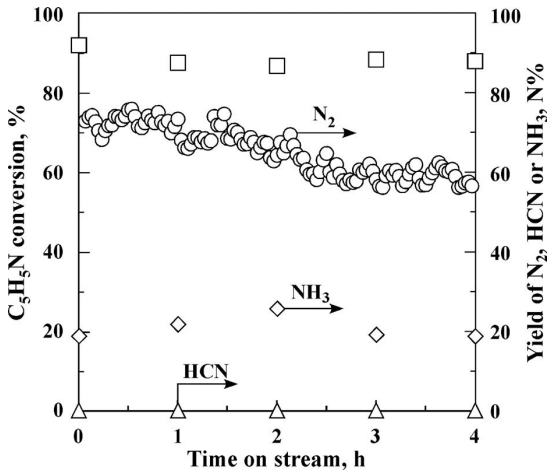


Fig. 6. Effect of 5% CO_2 addition on C_5H_5N decomposition under flowing 50% H_2/30% CH_4/5% CO at 850°C.

© 2016 ISIJ

of Eq. (1)) may lead to the increased activity at high temperatures of ≥ 850°C. The ΔG values for the Boudouard reaction at 750–950°C are estimated to be −2.1 to −10 kcal/mol, and the driving force is thus larger at a higher temperature.

3.4. Iron Forms of the Limonite after Reaction

As described above, the co-feeding of 20% CO/10% H_2 at 750°C or 50% H_2/30% CH_4/5% CO at 850°C with 100 ppmv C_5H_5N lowered the catalytic performance of the limonite considerably compared with the observation in inert He (Table 1, Figs. 1 and 5). On the other hand, the addition of H_2O or CO_2 to the syngas and main COG composition restored the catalytic activity (Figs. 2, 4 and 6). The used limonite catalysts were thus subjected to the XRD measurements to identify crystalline forms of Fe species. The α-FeOOH in as-received limonite was transformed into α-Fe with the average crystalline size of 25 nm after H_2 reduction.[25] **Figure 7** presents the XRD profiles for the limonite used in the presence of fuel gas components. As seen in Fig. 7(a), α-Fe was transformed predominantly into Fe_3C after C_5H_5N decomposition at 750°C in the coexistence of syngas alone. The formation of Fe_3C may be expressed as follows:

$$3Fe + C \rightarrow Fe_3C \quad \text{..... (5)}$$

The ΔG value for Eq. (5) at 750°C is calculated to be 0.2 kcal/mol. The carbide species may also be produced by the direct reaction (Eq. (6)) of α-Fe with CO fed.

$$3Fe + 2CO \rightarrow Fe_3C + CO_2 \quad \text{..... (6)}$$

The ΔG for Eq. (6) at 750°C is 2.3 kcal/mol, which means that the driving force for Eq. (6) is smaller than that for Eq. (5). Thus, Eq. (5) may be likely to be the main reaction for the formation of Fe_3C. It may therefore be reasonable to see that carbon formed by Eq. (1) and/or CO coexisted react with catalytically active α-Fe to provide Fe_3C, which causes the deactivation of the limonite catalyst.

When 3% H_2O or 10% CO_2 was added to syngas at 750°C, the XRD peaks attributable to Fe_3C and crystallized carbon disappeared almost completely, and α-Fe became the main species (Figs. 7(b) and 7(d)). The similar XRD profile was also observed with the used limonite after the reaction at 850°C in the CO_2-containing syngas (Fig. 7(e)). The disappearance of Fe_3C may be ascribed to the suppression of carbon deposition (Eq. (1)) by CO_2 coexisted or produced through Eq. (2), the gasification of C_5H_5N-derived carbon by the Boudouard reaction or H_2O coexisted (the reverse reaction of Eqs. (1) or (3), respectively), and/or the transformation of Fe_3C into α-Fe by the reaction of Fe_3C with H_2O (Eq. (7)) or CO_2 (Eq. (8)).

$$Fe_3C + H_2O \rightarrow 3Fe + CO + H_2 \quad \text{..... (7)}$$

$$Fe_3C + CO_2 \rightarrow 3Fe + 2CO \quad \text{..... (8)}$$

The ΔG values for Eqs. (7) and (8) at 650–850°C are estimated to be 0.1 to −5.8 and 1.4 to −6.1 kcal/mol, respectively. It is thus probable that the two oxidizing gases can protect catalytically active α-Fe from being carbonized and/or covered with deposited carbon, and the extent of the protection is larger at a higher temperature. After C_5H_5N decomposition at 650°C in 10% CO_2-containing syngas, as seen in Fig. 7(c), the diffraction peaks of Fe_3C and crystallized carbon were detected, whereas α-Fe did not appear. The reason may be that the driving force (ΔG = −2.1 kcal/mol) for Eq. (1) at 650°C is larger than that (ΔG = 1.4 kcal/mol) for Eq. (8) at this temperature.

Figure 8 illustrates the XRD patterns for the limonite used in the coexistence of COG components. After the decomposition reaction at 850°C in 50% H_2/30% CH_4/5%

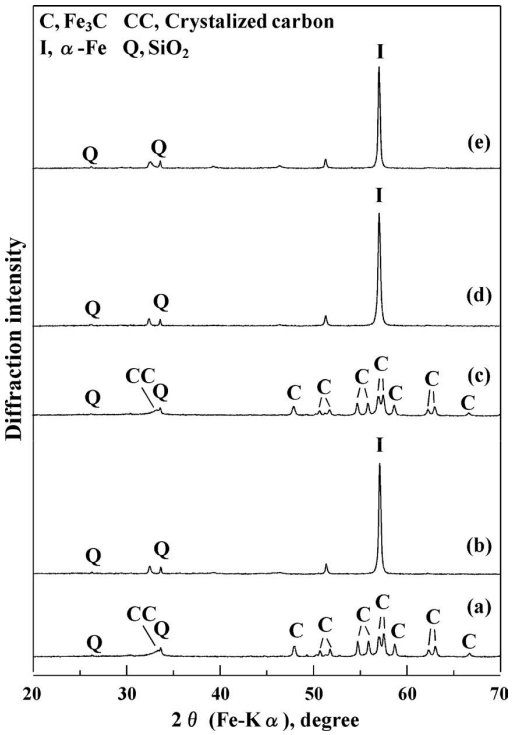


Fig. 7. XRD profiles for limonite samples after C_5H_5N decomposition in syngas/He at 750°C (a), H_2O/syngas/He at 750°C (b) and CO_2/syngas/He at 650°C (c), 750°C (d) and 850°C (e).

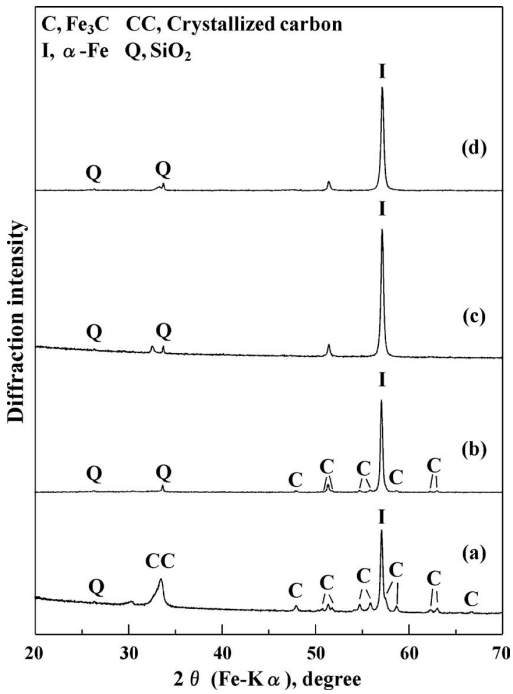


Fig. 8. XRD profiles for limonite samples after C_5H_5N decomposition in 50% H_2/30% CH_4/5% CO/He at 850°C (a) and 50% H_2/30% CH_4/5% CO/5% CO_2/He at 750°C (b), 850°C (c) and 950°C (d).

© 2016 ISIJ

CO, the XRD signals attributable to α-Fe, Fe_3C and crystallized carbon appeared (Fig. 8(a)). The ΔG values for the CO disproportionation (Eq. (1)) and the methane decomposition (Eq. (4)) reactions at 850°C are calculated to be 6.3 and −7.8 kcal/mol, respectively. The crystallized carbon is considered to be predominantly formed via Eq. (4). On the other hand, the formation of Fe_3C may proceed through the following equation (Eq. (9)) in addition to reactions involving deposited carbon (Eq. (5)) and/or CO (Eq. (6)).

$$3Fe + CH_4 \rightarrow Fe_3C + 2H_2 \quad \text{..... (9)}$$

The ΔG value for Eq. (9) at 850°C is −8.0 kcal/mol, which is lower than that for Eq. (5) ($\Delta G = -0.2$ kcal/mol) or 6 ($\Delta G = 6.1$ kcal/mol) at 850°C. It is thus likely that the catalyst deactivation observed in Fig. 5 comes mainly from the occurrence of Eq. (4) and/or Eq. (9).

When 5% CO_2 was added to 50% H_2/30% CH_4/5% CO above 850°C, the diffraction lines of crystallized carbon and Fe_3C disappeared almost completely, and α-Fe became the predominant Fe form (Figs. 8(c) and 8(d)). The disappearance of the former two species may be ascribed to the suppression of carbon formation (Eq. (1)) by CO_2 coexisted, the CO_2 gasification of CH_4- and C_5H_5N-derived carbonaceous materials (the reverse reaction of Eq. (1)), and/or the transformation of Fe_3C into α-Fe by the reaction between Fe_3C and CO_2 (Eq. (8)). On the basis of the above-mentioned results, it is evident that the coexistence of CO_2 can suppress the deactivation of the limonite catalyst in 50% H_2/30% CH_4/5% CO at $\geq$ 850°C. At 750°C, as seen in Fig. 8(b), the weak XRD peaks of Fe_3C were observed. This may be ascribed to a lower driving force for the Boudouard reaction (the reverse reaction of Eq. (1)) at 750°C compared with those at 850 and 950°C (section 3.3).

To clarify the mechanism of the limonite-catalyzed N_2 formation from C_5H_5N in the coexistence of fuel gas or COG components should be the subject of future work from a scientific point of view.

4. Conclusions

Catalytic decomposition of 100 ppmv C_5H_5N in the presence of fuel gas or COG components with limonite rich in α-FeOOH has been studied mainly with a cylindrical quartz reactor under the conditions of 0.1 MPa, 750–850°C and 51 000 h^{-1}. The principal conclusions are summarized as follows:

(1) The limonite catalyst exhibits very high activity for the decomposition of C_5H_5N in inert He at 500–850°C, and C_5H_5N conversion and N_2 yield at 500°C reach almost 100% and more than 85 N%, respectively.

(2) In the coexistence of 20% CO/10% H_2 at 750°C or 50% H_2/30% CH_4/5% CO at 850°C, the limonite is considerably deactivated due to the remarkable occurrence of carbon deposition.

(3) On the other hand, the addition of 5–10% CO_2 to the syngas and main COG composition can suppress carbon formation and consequently improve the catalytic activity of the limonite significantly.

(4) The XRD analyses reveal the transformation of α-FeOOH-derived active α-Fe into Fe_3C in the coexistence of 20% CO/10% H_2 alone or 50% H_2/30% CH_4/5% CO alone. When the H_2O or CO_2 is added to the syngas at 750°C and the main COG composition at 850°C, on the other hand, α-Fe is the only Fe form.

(5) On the basis of the above-mentioned results, it is likely that the two oxidizing gases can work for keeping the limonite surface as catalytically active α-Fe.

Acknowledgments

The present study was supported in part by the Steel Foundation for Environmental Protection Technology (SEPT). The authors acknowledge the supply of limonite from Kobe Steel Ltd and Mitsubishi Chemical Corp. in Japan.

REFERENCES

1) A. Tsutsumi: *CCT J.*, **11** (2004), 17.
2) S. C. Mitchell: Hot Gas Cleanup of Sulfur, Nitrogen, Minor and Trace Elements, IEA Coal Research, London, (1998), CCC/12.
3) S. Benson: Fuel Cells – Use with Coal and Other Solid Fuels, IEA Coal Research, London, (2001), CCC/47.
4) E. Suzuki: Proc. 2003 Gasification Technologies Conf., Gasification Technology Council, Arlington, (2003), 11.
5) MEGA-GSP Technology, Future Energy GmbH, Freiberg, (2005), 10.
6) C. Henderson: Clean Coal Technologies, IEA Coal Research, London, (2003), CCC/74.
7) N. Holt: Proc. 2004 Gasification Technologies Conference, Gasification Technologies Council, Arlington, (2004), 25.
8) S. J. Mills: Coal Gasification and IGCC in Europe, IEA Coal Research, London, (2006), CCC/113.
9) K. V. Thambimuthu: Gas Cleaning for Advanced Coal-Based Power Generation, IEA Coal Research, London, (1993), IEACR/53.
10) A. Dittler, G. Hemmer and G. Kasper: High Temperature Gas Cleaning, vol. II, G. Braun ems Gmbb, Karlsruhe, (1999).
11) T. Aramaki: *J. Jpn. Inst. Energy*, **85** (2006), 342.
12) K. Miura, M. Kawase, H. Nakagawa, R. Ashida, T. Nakai and T. Ishikawa: *J. Chem. Eng. Jpn.*, **36** (2003), 735.
13) M. Onozaki, K. Watanabe, T. Hashimoto, H. Saegusa and Y. Katayama: *Fuel*, **85** (2006), 143.
14) L. Li, K. Morishita and T. Takarada: *J. Chem. Eng. Jpn.*, **39** (2006), 461.
15) H. Cheng, X. Lu, X. Liu, Y. Zhang and W. Ding: *J. Nat. Gas Chem.*, **18** (2009), 467.
16) N. Tsubouchi, Y. Mochizuki, Y. Ono, K. Uebo, N. Sakimoto and T. Takahashi: *Energy. Fuels.*, **27** (2013), 7330.
17) Y. Ohtsuka, C. Xu, D. Kong and N. Tsubouchi: *Fuel*, **83** (2004), 685.
18) C. Xu, N. Tsubouchi, H. Hashimoto and Y. Ohtsuka: *Fuel*, **84** (2005), 1957.
19) N. Tsubouchi, H. Hashimoto and Y. Ohtsuka: *Catal. Lett.*, **105** (2005), 203.
20) N. Tsubouchi, H. Hashimoto and Y. Ohtsuka: Catalytic Decomposition of Ammonia in Fuel Gas Components with Inexpensive Limonite at High Temperatures, eds. by C. Kanaoka, H. Makino and H. Kamiya, Advanced Gas Cleaning Technology, Jugei Shobo, Tokyo, (2005), 483.
21) N. Tsubouchi, H. Hashimoto and Y. Ohtsuka: *Energy. Fuels.*, **21** (2007), 3063.
22) N. Tsubouchi, H. Hashimoto and Y. Ohtsuka: *Powder Technol.*, **180** (2008), 184.
23) Y. Ohtsuka, N. Tsubouchi, T. Kikuchi and H. Hashimoto: *Powder Technol.*, **190** (2009), 340.
24) T. Matsuyama, N. Tsubouchi and Y. Ohtsuka: *J. Mol. Catal. A-Chem.*, **356** (2012), 14.
25) N. Tsubouchi, A. Ogawa and Y. Mochizuki: *Appl. Catal. A-Gen.*, **499** (2015), 133.
26) N. Tsubouchi, H. Hashimoto and Y. Ohtsuka: *J. Mol. Catal. A-Chem.*, **407** (2015), 75.
27) A. E. Axworthy, V. H. Dayan and G. B. Martin: *Fuel*, **57** (1978), 29.
28) K. Murakami, M. Sato, K. Sugawara, N. Tsubouchi and Y. Ohtsuka: Proc. 48th Conf. Japan Institute of Energy for Coal Science, JIE, Tokyo, (2011), 94.

© 2016 ISIJ